Effects of Interparticle Attractions on Colloidal Sedimentation

A. Moncho-Jordá,[1] A. A. Louis,[2] and J. T. Padding[3]

[1]Departamento de Física Aplicada, Facultad de Ciencias, Universidad de Granada, Campus Fuentenueva S/N, 18071 Granada, Spain
[2]Rudolf Peierls Centre for Theoretical Physics, University of Oxford, 1 Keble Road, Oxford OX1 3NP, United Kingdom
[3]Computational Biophysics, University of Twente, P.O. Box 217, 7500 AE, Enschede, The Netherlands

(Received 15 June 2009; published 11 February 2010)

We use a mesoscopic simulation technique to study the effect of short-ranged interparticle attractions on the steady-state sedimentation of colloidal suspensions. Attractions increase the average sedimentation velocity v_s compared to the pure hard-sphere case, and for strong enough attractions, a nonmonotonic dependence on the packing fraction ϕ with a maximum velocity at intermediate ϕ is observed. Attractions also strongly enhance hydrodynamic velocity fluctuations, which show a pronounced maximum size as a function of ϕ. These phenomena arise from a complex interplay between nonequilibrium hydrodynamic effects and the thermodynamics of transient cluster formation.

DOI: 10.1103/PhysRevLett.104.068301 PACS numbers: 82.70.Dd, 05.40.−a, 47.11.−j

Many industrial applications of colloidal suspensions depend critically on their behavior under nonequilibrium conditions. Such properties are, however, notoriously hard to calculate because of long-ranged solvent induced hydrodynamic interactions (HI) [1]. Partially for this reason, the vast majority of theoretical and computational treatments of the nonequilibrium regime have focused on hard-sphere (HS) particles. Thus our understanding of how attractive interparticle interactions affect the nonequilibrium behavior of colloidal suspensions is still in its infancy. This state of affairs stands in marked contrast to the equilibrium regime, where methods to calculate how interactions control phase behavior and interfacial properties are already well developed [2].

To address this fundamental question, we study the effect of attractive interactions on a classic problem of nonequilibrium physics, namely, the steady-state sedimentation of spherical particles through a viscous solvent at low Reynolds number [1,3]. Besides its intrinsic interest for statistical mechanics, sedimentation is also important for understanding industrial applications such as paints, coatings, ceramics, food, and cosmetics [1].

Studies of sedimenting HS systems have shown that HI produce many rich and subtle effects [1,3]. Even just three sedimenting particles can exhibit chaotic behavior [4]. HI strongly influence the average sedimentation velocity v_s, which rapidly decreases with increasing packing fraction ϕ [5]. Scaling arguments suggest that velocity fluctuations around the average $\delta v = v - v_s$ are even more strongly affected by HI, and that they could diverge with container size L as $\langle(\delta v)^2\rangle \sim L$ [6]. This surprising prediction stimulated a large amount of research on these intrinsically chaotic hydrodynamic velocity correlations (swirls). Experiments show that the swirls do grow with container size for smaller L (the unscreened regime) and then saturate for larger containers (the screened regime) [7], but the nature and origins of the screening are still a source of controversy [3,8–11]. Here we explore how these subtle hydrodynamic phenomena change when a new thermodynamic component, in the form of interparticle attractions, is added to the mix. We find a rich interplay between the thermodynamics of cluster formation and nonequilibrium hydrodynamics.

In a seminal paper, Batchelor calculated the effect of interparticle attractions beyond the HS model on the average sedimentation velocity in the dilute limit [12]; for short-ranged potentials this gives [1]:

$$v_s/v_s^0 \approx 1 - [6.55 - 3.52(1 - B_2^*)]\phi + \mathcal{O}(\phi^2), \quad (1)$$

where v_s^0 is the sedimentation velocity of a single colloid, $B_2^* \equiv B_2/B_2^{\mathrm{HS}}$, B_2 is the second virial coefficient, and B_2^{HS} is the virial coefficient calculated with the effective HS radius of the colloids. Equation (1) suggests that attractions should increase the sedimentation velocity, while added repulsions should decrease it compared to the pure HS case. Experiments on dilute suspensions with intercolloid attractions [13,14] or long-ranged electrostatic repulsions [15] are consistent with this picture. However, these theories and experiments are only relevant in the dilute limit. What happens to the average sedimentation velocity at larger volume fractions is not well understood, and virtually nothing is known about the effect of attractions on velocity fluctuations.

We address these questions by applying a mesoscopic simulation technique based on stochastic rotation dynamics (SRD) [16,17], that can successfully reproduce hydrodynamic fluctuations in steady-state sedimentation [18] and has recently been shown to *quantitatively* describe colloidal sedimentation experiments, including complex nonlinear effects such as Rayleigh Taylor instabilities [19]. The accuracy with which SRD was shown to reproduce colloidal experiments gives us confidence in the predictions of our simulations with interparticle attractions. We are able to go beyond the dilute regime and

find that, for short-ranged attractive potentials, Eq. (1) is accurate up to about $\phi \approx 0.05$, but breaks down for higher packing fractions. We measure, for the first time, the effect of attractions on velocity fluctuations in the unscreened regime, and find that the range of the hydrodynamic swirls is greatly increased by attractions, with a maximum around $\phi \approx 0.07$ for stronger attractions. We link the increase in both average sedimentation velocity and in the size of the hydrodynamic swirls to a complex interplay between the aggregation, fragmentation, and sedimentation of transient clusters.

In our simulations, the colloid-colloid interaction was modeled by a classic DLVO [1] potential: $V_{cc}(r) = V_{HS}(r) + V_{vdW}(r) + V_{DH}$. The first term is a repulsive HS like contribution: $\beta V_{HS}(r) = 10[(\sigma/r)^{2n} - (\sigma/r)^n + 1/4]$ for $r \leq 2^{1/n}\sigma$ and 0 for $r > 2^{1/n}\sigma$, where $n = 24$ and $\sigma = \sigma_{cc}$, the colloidal HS radius. The second and third terms are the short-range van der Waals attraction and the repulsive Debye-Hückel-like contribution respectively [1]; their exact forms are taken from Ref. [20]; we include, as they do, a cutoff distance (Stern layer) given by $\delta = 0.048\sigma_{cc}$ to overcome the van der Waals singularity. Keeping the Debye screening length fixed at $\kappa = 8.96/\sigma_{cc}$, we varied the Hamaker constant and particle charge to obtain four different potentials with an attractive minimum at short interparticle distance. The normalized second virial coefficients were $B_2^* = -0.063$, -0.507, -1.044, and -1.416, respectively. Note that all these values are above $B_2^* = -1.5$ to avoid fluid-fluid phase separation [21].

Brownian fluctuations and HI are induced by SRD fluid particles that interact with each other through an efficient coarse-grained collision step that conserves mass, energy, and momentum, so that the Navier-Stokes equations are recovered at the macroscopic level [16]; note that in the literature this method is also called multiple particle collision dynamics and has been widely applied to soft-matter simulations [22]. The colloids couple to the SRD fluid through an interaction of the form $\beta V_{cf}(r) = 10[(\sigma/r)^{2n} - (\sigma/r)^n + 1/4]$ for $r \leq 2^{1/n}\sigma$ and 0 for $r > 2^{1/n}\sigma$, where $n = 6$ and $\sigma = \sigma_{cf} = 0.465\sigma_{cc}$. The equations of motion are updated with a standard molecular dynamics algorithm for the colloid-colloid and the colloid-fluid interactions, and with a coarse-grained SRD collision step for the fluid-fluid interactions. The colloid-fluid diameter σ_{cf} is lightly smaller than $0.5\sigma_{cc}$ to avoid spurious depletion forces between the colloids [17,18]. This mesoscopic simulation technique has been shown to reproduce the correct low Reynolds (Re) hydrodynamic flow behavior with an effective hydrodynamic radius of $a \approx 0.8\sigma_{cf}$, as well as the correct thermal Brownian fluctuations and diffusion for colloidal suspensions. See Refs. [17,18] for further technical details and a justification of our SRD parameter choice.

The simulations were performed by placing $N_c = 8$–819 colloids in a box of sizes $L_x = L_y = 16\sigma_{cf}$ and $L_z = 48\sigma_{cf}$ with periodic boundary conditions. The number of solvent particles was $N = 40V_{free}/\sigma_{cf}^3 \sim 4 - 5 \times 10^5$, where V_{free} is the free volume left by the colloids. A gravitational external field g is applied to the colloids in the z direction in order to induce sedimentation. After an initial transient time, the system reaches steady-state conditions, where the average sedimentation velocity v_s is constant, the one-body particle spatial distribution is homogeneous, and no drift is observed.

The simulation box sizes are small enough that we are still in the unscreened regime [18]; larger simulations and possibly different boundary conditions [9,10] are necessary in order to observe screening. The particle Re number $\mathrm{Re} = v_s a/\nu$, where ν is the kinematic viscosity, was kept at $\mathrm{Re} \approx 0.08$, which is small enough for the system to be in the correct low Re number Stokesian regime. Similarly, the Péclet number $\mathrm{Pe} = v_s^0 a/D_c$, with D_c the equilibrium colloid self-diffusion coefficient, was $\mathrm{Pe} = 2.5$, so that thermal Brownian noise is nonnegligible.

We begin our study with the effect of the interparticle attractions on the average sedimentation velocity. Figure 1 shows v_s for various attractions and for different packing fractions $\phi = \frac{4}{3}\pi\rho a^3$, where ρ is the colloid number density. Note that for these hydrodynamic effects, the correct radius to use is the hydrodynamic one. In the dilute limit, the simulation results are well described by Batchelor's prediction (1) with no free parameters. For $B_2^* > -0.86$ the slope at low ϕ is negative, but for $B_2^* < -0.86$ the attractions become strong enough to overcome the backflow-induced velocity reduction and give rise to a positive slope. These results suggest that, at least for short-ranged attractions, the exact potential details are unimportant and v_s/v_s^0 is controlled by B_2.

At larger packing fractions the Batchelor prediction (1) breaks down. Interestingly, for more attractive systems ($B_2^* < -0.86$) there is a clear maximum in v_s vs ϕ that

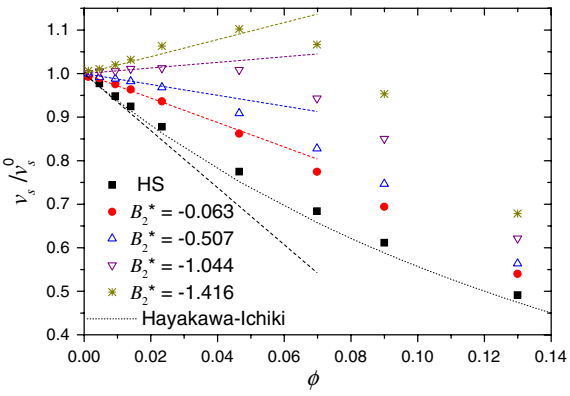

FIG. 1 (color online). Average sedimentation velocity v_s as a function of the volume fraction $\phi = \frac{4}{3}\pi\rho a^3$ for four different interparticle attractions and for hard spheres. The dashed lines are Batchelor's predictions (1) for the dilute limit. The dotted line is a prediction known to be accurate for hard spheres [23].

becomes more pronounced for stronger attractions. To our knowledge, such a nonmonotonic dependence on ϕ has not been observed before in simulations.

Next we investigate how attractions affect the velocity fluctuations of the particles around the average, $\delta v = v - v_s$. Here we focus on spatial correlations in the z direction, defined as $C_z(\vec{r}) = \langle \delta v_z(0) \delta v_z(\vec{r}) \rangle / \langle \delta v_z(0)^2 \rangle$, where $\langle \ldots \rangle$ is the average over time and over all colloids. The distance vector $\vec{r}$ can be parallel to the sedimentation, $C_z(z)$, or perpendicular to it, $C_z(x)$. The correlation function $C_z(z)$ exhibits an exponential decay $C_z(z) = \exp(-z/\xi_\parallel)$, where $\xi_\parallel$ is the correlation length in the direction parallel to the sedimentation. It provides a measure of the hydrodynamic swirl size. $C_z(x)$ decays as well, but also shows an anticorrelation region where the swirl moves in the opposite direction. The qualitative shape and decay of the swirls is similar to that seen in experiments [7] and simulations [18] for HS particles. However, as can be seen in Fig. 2, the correlation length $\xi_\parallel$ is greatly enhanced by the attractions. Whereas for weaker attractions $\xi_\parallel$ decreases with ϕ, similar to what is observed for HS particles [7,18], for more strongly attractive systems the correlation length first increases with ϕ and then decreases, giving rise to a maximum around $\phi \approx 0.07$ for $B_2^* < -1$. A similar nonmonotonic behavior with ϕ is observed for $C_z(x)$ (not shown).

To explain the effect of the interactions on the sedimentation, we first note that although the attractions in our system are not strong enough to form permanent clusters, they do enhance the probability for particles to cluster together in a transient fashion. This effect can be clearly seen in Fig. 3 where we plot the probability distribution of transient clusters $P(i)$ and their average lifetime $\tau(i)$ as a function of the cluster size, i. In order to distinguish whether a pair of particles belong to the same cluster or not, a cutoff distance $r_{\text{cut}} = 1.06\sigma_{\text{cc}}$ was used, which is a reasonable estimate of the range of the attractive potential well. We checked that our results do not qualitatively depend on the exact cutoff distance r_{cut}. As the attraction strength increases, both the probability of finding clusters $[P(i > 1)]$ and the average cluster lifetime $\tau(i)$ increases. The gravitational force on a cluster increases linearly with the number of particles inside the cluster, but the friction increases roughly linearly with the radius of gyration of the cluster. Since the latter typically increases less quickly than the former, larger clusters sediment faster than smaller ones, an effect we observe by tracking the clusters in time. Furthermore, we find that stronger interactions lead to slightly more compact clusters, with a smaller radius of gyration and so even larger sedimentation velocities.

Taken together, these cluster effects help explain why at a fixed ϕ, increasing the strength of the attractions increases the average sedimentation velocity v_s. Furthermore, faster clusters with a longer lifetime are able to move along larger distances with a roughly constant velocity. This leads to the propagation of the correlations along larger distances and so, to an increase of $\xi_\parallel$.

To examine the effect of changing ϕ, we show, in Fig. 4, how the cluster distribution changes when varying ϕ at a fixed attraction. The curves show the same qualitative behavior for all the B_2: as ϕ increases, the particles are on average closer to one another, and so the probability of being in a cluster grows. When the gaps between particles are large (low ϕ), the enhanced transient cluster formation at strong attractions leads to an increase in v_s and $\xi_\parallel$. On the other hand, if the gap between nearest neighbors is much less than the particle radius, then the fluid flow must be squeezed through the interparticle voids, leading to a decrease of v_s with ϕ that resembles that of pure HS

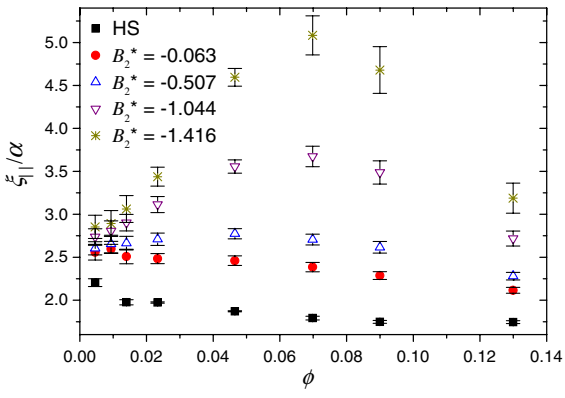

FIG. 2 (color online). Correlation length $\xi_\parallel$ parallel to the sedimentation direction for velocity swirls, as a function of packing fraction ϕ for different interparticle attractions and for pure HS. Attractions strongly enhance the size of the velocity swirls.

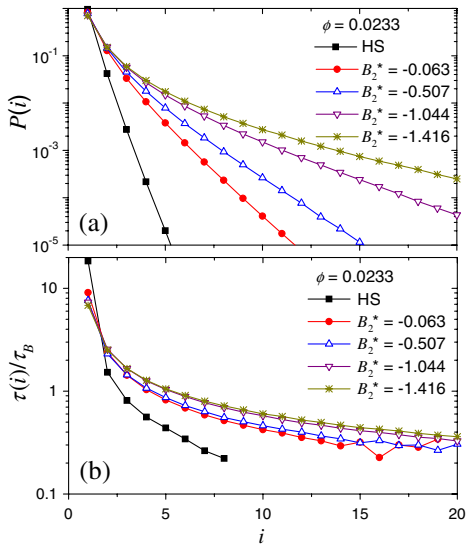

FIG. 3 (color online). (a) The probability of finding a transient cluster of size i and (b) the average cluster lifetime (normalized by the Brownian time $\tau_B = a^2/D_c$ as a function of i for hard spheres and for four different interparticle attractions. The particle volume fraction is $\phi = 0.0233$.

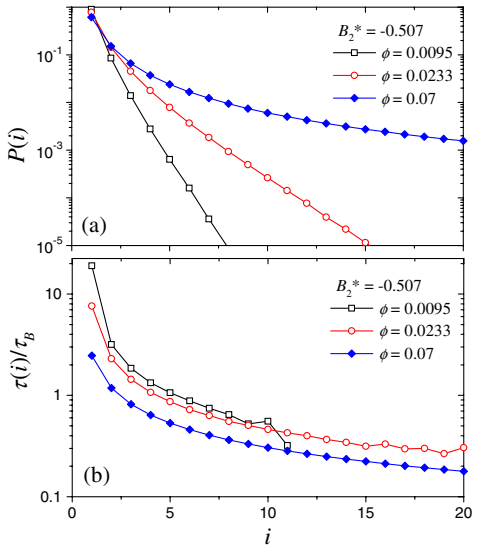

FIG. 4 (color online). The plots show (a) the probability of finding a transient cluster of size i and (b) the average cluster lifetime (normalized by the Brownian time τ_B) as a function of i for three different particle volume fractions, ϕ. The normalized second virial coefficient is $B_2^* = -0.507$.

systems. We estimate that a maximum in v_s/v_0 will occur when the typical gap width is about one radius; i.e., the average interparticle distance between particle centers is $d = 3a$. Assuming that the average interparticle distance is given by $d \sim a\phi^{-1/3}$, this corresponds to a volume fraction $\phi = (a/d)^3 \approx 0.04$, which agrees qualitatively with the $\phi \approx 0.05$ we find.

Calculating velocity fluctuations is notoriously subtle [3,6–11,18]. Nevertheless, the cluster picture can shed some light. From Fig. 4(b) we see that the clusters have a shorter lifetime for larger ϕ, presumably because the collision rate with other particles increases. This decreases $\xi_\parallel$. In addition, the fluctuations tend to track v_s, so when this decreases, they also decrease. At low ϕ and stronger attractions, the enhanced transient cluster formation wins out, but at higher ϕ the shorter cluster lifetimes and backflow-induced reduction of v_s dominate. The competition between these effects helps to qualitatively explain the nonmonotonic behavior of $\xi_\parallel$ with ϕ.

Finally, this study also raises a number of further questions. First, it would be interesting to see what happens for larger Pe numbers. Preliminary simulations up to Pe = 15 show that larger clusters are slightly less likely to occur at higher Pe numbers, most likely because the enhanced shear forces break them up, leading to slightly lower sedimentation velocity ratios v_s/v_0.

Second, it would be very interesting to study larger box sizes, to see whether attractions alter the crossover from the screened to the unscreened regime. Third, for even stronger attractions ($B_2^* < -1.5$) permanent clusters should begin to form. These will then sediment more quickly than monomers. But as they grow and accelerate, at some point the shear forces should break them up again. Such a rich interplay between aggregation and hydrodynamics should lead to new steady states with a cluster population that depends on the attraction strength. New simulations are planned to address these questions that not only have many practical applications for colloids, but also demonstrate the rich complexity of combining thermodynamics with nonequilibrium physics.

The authors thank the Spanish Ministerio de Ciencia e Innovación (Project No. MAT2009-13155-C04-02), the Junta de Andalucía (Project No. P07-FQM-02517), the Royal Society (London), and the Netherlands Organization for Scientific Research (NWO) for financial support.

[1] W. B. Russel, D. A. Saville, and W. R. Showalter, *Colloidal Dispersions* (Cambridge Univ. Press, Cambridge, U.K., 1989).
[2] C. N. Likos, Phys. Rep. **348**, 267 (2001).
[3] S. Ramaswamy, Adv. Phys. **50**, 297 (2001).
[4] I. M. Jánosi, T. Tél, D. E. Wolf, and J. A. C. Gallas, Phys. Rev. E **56**, 2858 (1997).
[5] G. K. Batchelor, J. Fluid Mech. **52**, 245 (1972).
[6] R. E. Caflisch and J. H. C. Luke, Phys. Fluids **28**, 759 (1985).
[7] H. Nicolai *et al.*, Phys. Fluids **7**, 12 (1995); P. N. Segrè, E. Herbolzheimer, and P. M. Chaikin, Phys. Rev. Lett. **79**, 2574 (1997).
[8] D. L. Koch and E. S. G. Shaqfeh, J. Fluid Mech. **224**, 275 (1991).
[9] A. J. C. Ladd, Phys. Rev. Lett. **88**, 048301 (2002).
[10] P. Mucha *et al.*, J. Fluid Mech. **501**, 71 (2004).
[11] B. U. Felderhof, Physica (Amsterdam) **387A**, 5999 (2008).
[12] G. K. Batchelor, J. Fluid Mech. **119**, 379 (1982).
[13] J. W. Jansen, C. G. de Kruif, and A. Vrij, J. Colloid Interface Sci. **114**, 501 (1986).
[14] K. L. Planken *et al.*, J. Phys. Chem. B **113**, 3932 (2009).
[15] D. M. E. Thies-Weesie *et al.*, J. Colloid Interface Sci. **176**, 43 (1995).
[16] A. Malevanets and R. Kapral, J. Chem. Phys. **110**, 8605 (1999).
[17] J. T. Padding and A. A. Louis, Phys. Rev. E **74**, 031402 (2006).
[18] J. T. Padding and A. A. Louis, Phys. Rev. Lett. **93**, 220601 (2004); Phys. Rev. E **77**, 011402 (2008).
[19] A. Wysocki *et al.*, Soft Matter **5**, 1340 (2009).
[20] G. Pellicane, D. Costa, and C. Caccamo, J. Phys. Condens. Matter **15**, 375 (2003).
[21] G. Vliegenthart and H. N. W. Lekkerkerker, J. Chem. Phys. **112**, 5364 (2000).
[22] G. Gompper, T. Ihle, D. M. Kroll, and R. G. Winkler, Adv. Polym. Sci. **221**, 1 (2009).
[23] H. Hayakawa and K. Ichiki, Phys. Rev. E **51**, R3815 (1995).